

# Dielectric and ferroelectric properties of lead magnesium niobate–lead zirconate titanate ceramics prepared by mixed-oxide method

R. Yimnirun<sup>a,\*</sup>, S. Ananta<sup>a</sup>, P. Laoratanakul<sup>b</sup>

<sup>a</sup> Department of Physics, Faculty of Science, Chiang Mai University, Chiang Mai 50200, Thailand

<sup>b</sup> National Metal and Materials Technology Center, Pathumthani 12120, Thailand

Received 11 May 2004; received in revised form 14 July 2004; accepted 25 July 2004

Available online 29 September 2004

## Abstract

The dielectric and ferroelectric properties of  $(x)\text{Pb}(\text{Mg}_{1/3}\text{Nb}_{2/3})\text{O}_3-(1-x)\text{Pb}(\text{Zr}_{0.52}\text{Ti}_{0.48})\text{O}_3$  (where  $x = 0, 0.1, 0.3, 0.5, 0.7, 0.9$ , and  $1.0$ ) ceramics prepared by an oxide-mixing method are measured by means of an automated dielectric measurement set-up and a modified Sawyer-Tower circuit, respectively. The dielectric properties of the ceramics are measured as functions of both temperature and frequency. The results indicate that the dielectric properties of the pure-phase PZT and PMN are of normal and relaxor ferroelectric behaviors, respectively. The dielectric behaviors of the 0.1PMN–0.9PZT and 0.3PMN–0.7PZT ceramics are more of normal ferroelectrics, while the other compositions are obviously of relaxor ferroelectrics. In addition, the transition temperature decreases and the maximum dielectric constant increases with increasing PMN content in the system. The  $P$ – $E$  hysteresis loop measurements demonstrate that the ferroelectric properties of the ceramics in PMN–PZT system change gradually from the normal ferroelectric behavior in PZT ceramic to the relaxor ferroelectric behavior in PMN ceramic. These results clearly show the significance of PMN in controlling the electrical responses of the PMN–PZT system.

© 2004 Elsevier Ltd. All rights reserved.

**Keywords:** Dielectric properties; Ferroelectric properties; Mixed-oxide; PMN–PZT

## 1. Introduction

Lead-based perovskite-type solid solutions consisting of the ferroelectric and relaxor materials have attracted a growing fundamental and practical interest because of their excellent dielectric, piezoelectric and electrostrictive properties which are useful in actuating and sensing applications. Among the lead-based complex perovskites, lead magnesium niobate ( $\text{Pb}(\text{Mg}_{1/3}\text{Nb}_{2/3})\text{O}_3$  or PMN) and lead zirconate titanate ( $\text{Pb}(\text{Zr}_{1-x}\text{Ti}_x)\text{O}_3$  or PZT) ceramics have been investigated extensively, both from academics and commercial viewpoints.<sup>1–3</sup> These two types of ceramics possess distinct characteristics that in turn make each ceramic suitable for different applications. With the complementary features of PMN and PZT described in many publications, the solid so-

lutions between PMN and PZT are expected to synergistically combine the properties of both normal ferroelectric PZT and relaxor ferroelectric PMN, which could exhibit better piezoelectric and dielectric properties than those of the single-phase PMN and PZT.<sup>4–10</sup> Furthermore, the properties can also be tailored over a wider range by changing the compositions to meet the strict requirements for specific applications.<sup>9–11</sup> In recent years, there have been several investigations on PMN–PZT system.<sup>4–14</sup> Many of these works have been on the PMNZT system, in which the starting oxide precursors were mixed together, and the ternary system of PMN–PZ–PT.<sup>4,5,13,15</sup> However, these previous works have only focused on a few compositions in the vicinity of the morphotropic phase boundary (MPB) and of the end members.<sup>1,8–10,12,14,16</sup> Thus far, there has been no systematic study on dielectric and ferroelectric properties of the ceramics within the entire compositional range between PMN and PZT at MPB composition; e.g.  $\text{Pb}(\text{Zr}_{0.52}\text{Ti}_{0.48})\text{O}_3$ .

\* Corresponding author. Tel.: +66 53943376; fax: +66 53357512.

E-mail address: [rattikor@chiangmai.ac.th](mailto:rattikor@chiangmai.ac.th) (R. Yimnirun).

Therefore, as an extension to the research on the PMN–PZT ceramics, the overall purpose of this study is to determine the temperature and frequency dependence of the dielectric properties and the ferroelectric behaviors of ceramics in the  $(x)\text{Pb}(\text{Mg}_{1/3}\text{Nb}_{2/3})\text{O}_3-(1-x)\text{Pb}(\text{Zr}_{0.52}\text{Ti}_{0.48})\text{O}_3$  (where  $x = 0, 0.1, 0.3, 0.5, 0.7, 0.9$ , and 1) binary system prepared by a conventional mixed-oxide method.

## 2. Experimental

The PMN–PZT ceramics used in this study are prepared from PMN and PZT starting powders. Initially, perovskite-phase PMN powders are obtained via a well-known columbite method, while PZT powders are prepared by a mixed-oxide method. With the columbite method, the magnesium niobate powders are first prepared by mixing starting  $\text{MgO}$  (>98%) and  $\text{Nb}_2\text{O}_5$  (99.9%) powders and then calcining the mixed powders at  $1050^\circ\text{C}$  for 2.5 h. This yields a so-called columbite powder ( $\text{MgNb}_2\text{O}_6$ ). The columbite powders are subsequently ball-milled with  $\text{PbO}$  (99%) for 24 h. The mixed powders are calcined at  $800^\circ\text{C}$  for 2.5 h to form a perovskite-phase PMN. With a more conventional oxide-mixing route, PZT powders are prepared from reagent-grade  $\text{PbO}$  (99%),  $\text{ZrO}_2$  (99%), and  $\text{TiO}_2$  (98.5%) starting powders. These powders are ball-milled for 24 h and later calcined at  $850^\circ\text{C}$  for 2 h. The  $(x)\text{Pb}(\text{Mg}_{1/3}\text{Nb}_{2/3})\text{O}_3-(1-x)\text{Pb}(\text{Zr}_{0.52}\text{Ti}_{0.48})\text{O}_3$  (where  $x = 0, 0.1, 0.3, 0.5, 0.7, 0.9$ , and 1.0) ceramic composites are then prepared from the PZT and PMN powders by the mixed-oxide method at various processing conditions. For optimization purpose, the sintering temperature is varied between  $1000^\circ\text{C}$  and  $1300^\circ\text{C}$  depending upon the compositions.<sup>6</sup>

The densities of the sintered ceramics are measured by Archimedes method. The firing shrinkage is determined from the dimensions of the specimens before and after the sintering process. The phase formations of the sintered specimens are studied by an X-ray diffractometer (Philips Analytical). The microstructure analyses are undertaken by a scanning electron microscopy (SEM: JEOL Model JSM 840A). Grain size is determined from SEM micrographs by a linear intercept method.

For electrical properties characterizations, the sintered samples are lapped to obtain parallel faces, and the faces are then coated with silver paint as electrodes. The samples are heat-treated at  $750^\circ\text{C}$  for 12 min to ensure the contact between the electrodes and the ceramic surfaces. The samples are subsequently poled in a silicone oil bath at a temperature of  $120^\circ\text{C}$  by applying a dc field of 25 kV/cm for 30 min and field-cooled to room temperature. The dielectric properties of the sintered ceramics are studied as functions of both temperature and frequency with an automated dielectric measurement system. The computer-controlled dielectric measurement system consists of a precision LCR-meter (Hewlett-Packard, model 4284A), a temperature chamber (Delta Design, model 9023), and a computer system. The ca-

pacitance and the dielectric loss tangent are determined over the temperature range of  $-150^\circ\text{C}$  and  $400^\circ\text{C}$  with the frequency ranging from 100 Hz to 1 MHz. The measurements are carried out on cooling continuously. Before each cooling run, the samples are first heated up to  $400^\circ\text{C}$  and then cooling run is performed at the rate of  $3^\circ\text{C}/\text{min}$ . The dielectric constant is then calculated from  $\epsilon_r = Cd/\epsilon_0A$ , where  $C$  is the capacitance of the sample,  $d$  and  $A$  are the thickness and the area of the electrode, respectively, and  $\epsilon_0$  is the dielectric permittivity of vacuum ( $8.854 \times 10^{-12}$  F/m). The ferroelectric hysteresis ( $P$ – $E$ ) loops are characterized by using a computer controlled modified Sawyer-Tower circuit. The high voltage is applied to a sample by a bipolar amplifier (Kepco, model 1000 M) and a high voltage AC amplifier (Trek, model 610C) with the input signals with a frequency of 0.1 Hz from a lock-in amplifier (Stanford Research System, model 830). The detailed descriptions of these systems are explained elsewhere.<sup>17,18</sup>

## 3. Results and discussion

The phase formation behavior of the sintered ceramics is revealed by an XRD method. The XRD patterns, shown in Fig. 1, show that the sintered ceramics are mainly in perovskite phase. From the XRD pattern, PZT ceramic is identified as a single-phase material with a perovskite structure

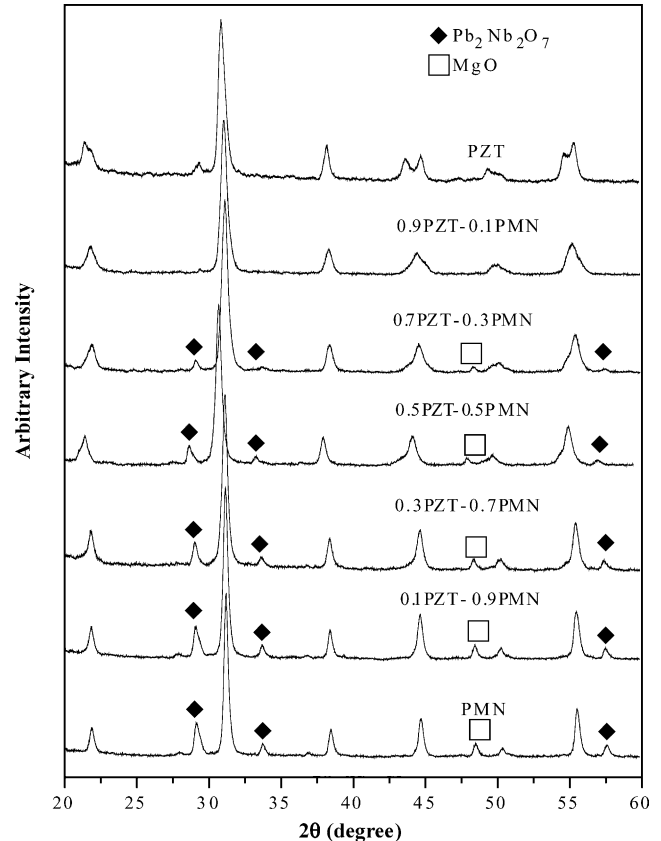


Fig. 1. XRD diffraction patterns of the sintered  $(x)\text{PMN}-(1-x)\text{PZT}$  ceramics.

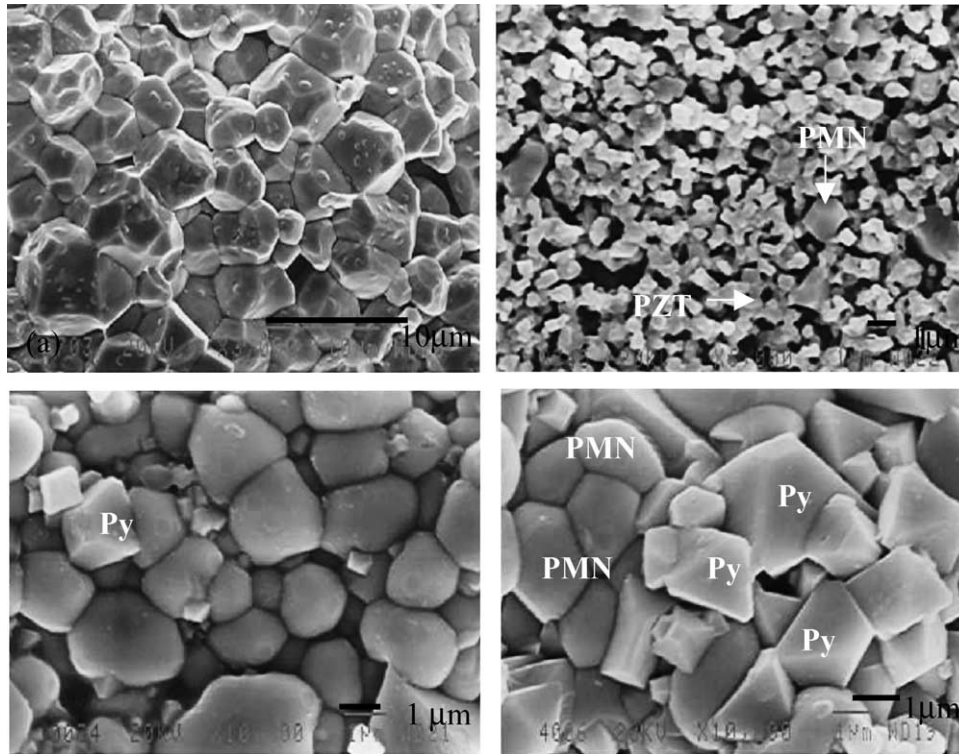


Fig. 2. SEM micrographs of  $(x)$ PMN– $(1 - x)$ PZT ceramics sintered at 1150 °C: (a) PZT, (b) 0.1PMN–0.9PZT, (c) 0.7PMN–0.3PZT, and (d) PMN (Py indicates pyrochlore phase).

having tetragonal symmetry, while PMN ceramic is a perovskite material with a cubic symmetry.<sup>8</sup> All PMN–PZT ceramic composites exhibit pseudocubic crystal structure, as reported in previous investigations.<sup>4,5,13</sup> However, some impurity phases ( $\text{Pb}_2\text{Nb}_2\text{O}_7$  and MgO) are also present on the XRD patterns of the composites with  $x > 0.1$ . The secondary pyrochlore phase ( $\text{Pb}_2\text{Nb}_2\text{O}_7$ ) is clearly present on the SEM micrographs as cubic particles, resulting in very heterogeneous microstructure (Fig. 2(c–d)). These impurity phases are believed to precipitate mostly on the surface areas of the specimens.<sup>19</sup> Further XRD investigation at different depths of the specimen reveals that the impurities diminish in the interior areas of the specimens.

The optimized density of sintered  $(x)$ PMN– $(1 - x)$ PZT ceramics is listed in Table 1. It is observed that the compositions with  $x = 0.1$  and 0.3 show relatively lower density than other compositions. This suggests that the addition of a small

amount of PMN to the PMN–PZT compositions results in a significant decrease in the density of the ceramics. Further addition of PMN into the compositions increases the density again. Similar result was reported in previous investigation.<sup>4</sup> The SEM investigations (Fig. 2) reveal supporting evidences that the ceramics with these two compositions contain very small and loosely bonded grains. It should, however, be noted that the composition with  $x = 0.1$ , which contains sub-micron size grains, is not well-sintered. Clearly, this is a reason for the much lower density in this composition. As shown in Table 1, the average grain size of all the mixed compositions is much smaller than that of the pure PZT and PMN materials. The grain size varies considerably from  $<1$  to 7  $\mu\text{m}$ . The reason for the changes of the density and the smaller grain sizes in the mixed compositions is not clearly understood, but this may be a result of PMN's role as a grain-growth inhibitor in the PMN–PZT composites.<sup>8</sup> More importantly, it should be pointed out that dense ceramics for PMN–PZT composites are very difficult to obtain as a result of a narrow range of sintering behavior of PMN material.<sup>4</sup> This is particularly critical in ceramics with high PMN content, which show very heterogeneous microstructure as a result of the secondary pyrochlore phase. This could very well be a limit of the mixed-oxide method at high PMN content, even when used in conjunction with a columbite-precursor method. As a result, many investigators have prepared better PMN–PZT ceramics by carefully controlling the Zr:Ti ratio, by using a combination of wet–dry methods, or by doping with other elements.<sup>4,5,8–10,12,14</sup>

Table 1  
Characteristics of PMN–PZT ceramics with optimized processing conditions

| Ceramic       | Density ( $\text{g}/\text{cm}^3$ ) | Grain size range ( $\mu\text{m}$ ) | Average grain size ( $\mu\text{m}$ ) |
|---------------|------------------------------------|------------------------------------|--------------------------------------|
| PZT           | $7.59 \pm 0.11$                    | 2–7                                | 5.23                                 |
| 0.1PMN–0.9PZT | $6.09 \pm 0.11$                    | 0.5–2                              | 0.80                                 |
| 0.3PMN–0.7PZT | $7.45 \pm 0.10$                    | 0.5–3                              | 1.65                                 |
| 0.5PMN–0.5PZT | $7.86 \pm 0.05$                    | 0.5–5                              | 1.90                                 |
| 0.7PMN–0.3PZT | $7.87 \pm 0.07$                    | 1–4                                | 1.40                                 |
| 0.9PMN–0.1PZT | $7.90 \pm 0.09$                    | 1–4                                | 1.50                                 |
| PMN           | $7.82 \pm 0.06$                    | 2–4                                | 3.25                                 |

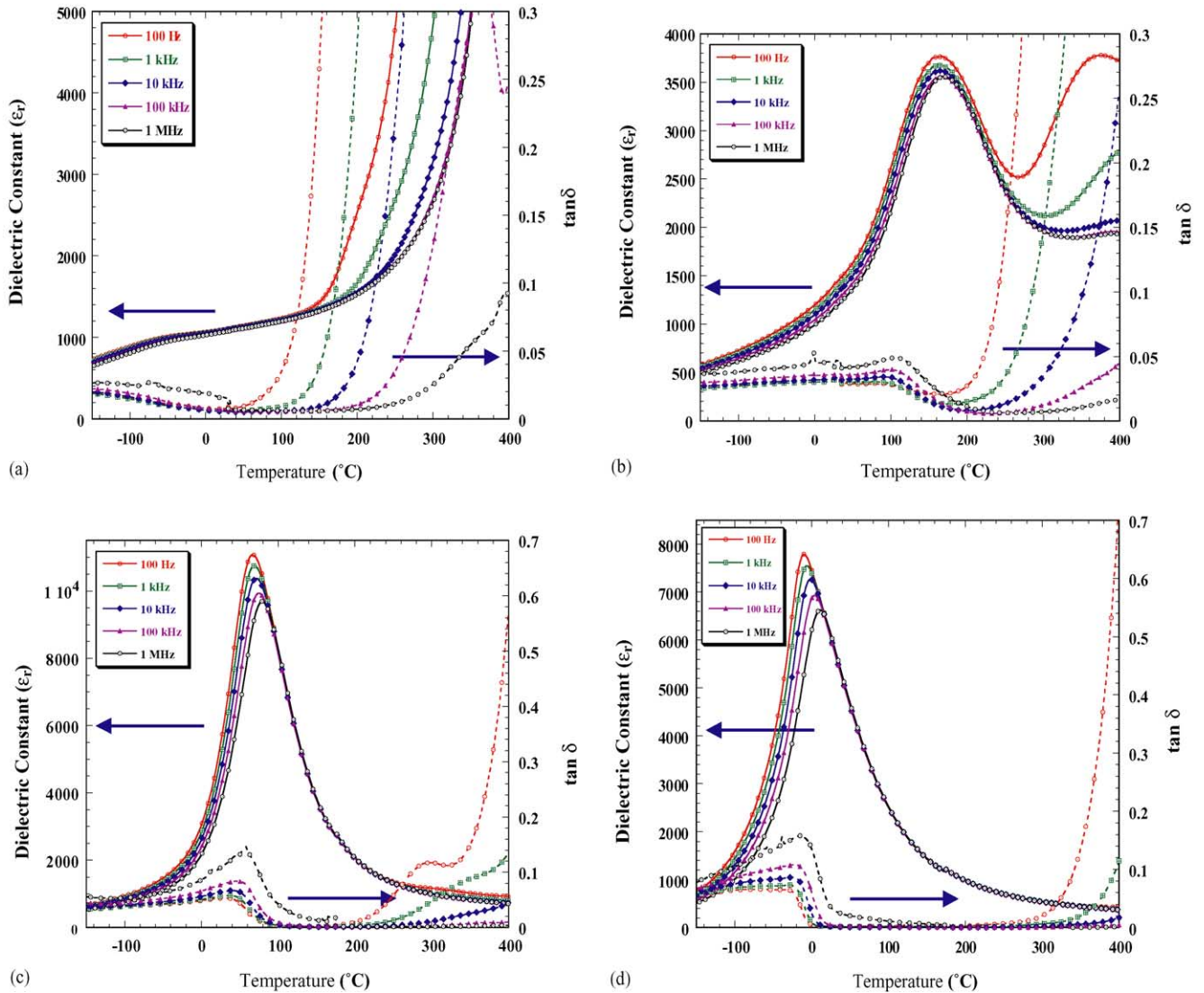


Fig. 3. (a) Temperature and frequency dependences of dielectric properties of PZT ceramic, (b) temperature and frequency dependences of dielectric properties of 0.3PMN–0.7PZT ceramic, (c) temperature and frequency dependences of dielectric properties of 0.7PMN–0.3PZT ceramic and (d) temperature and frequency dependences of dielectric properties of PMN ceramic.

The dielectric properties, e.g. dielectric constant ( $\epsilon_r$ ) and  $\tan \delta$ , are measured as functions of both temperature and frequency, as shown in Fig. 3(a–d). As listed in Table 2, except for PZT the maximum dielectric constant increases steadily with increasing PMN content ( $\epsilon_r$  increases from  $\sim 3700$  in

0.1PMN–0.9PZT to  $\sim 10700$  in 0.9PMN–0.1PZT). The PMN is expected to show larger value of the dielectric constant, but the lower value is attributed to the detrimental effect of the secondary pyrochlore phase.<sup>16</sup> The dielectric properties of PZT ceramic, as plotted in Fig. 3(a), change significantly

Table 2  
Dielectric properties of (x)PMN–(1–x)PZT ceramics (at 1 kHz)

| Ceramic       | $T_C$ (°C) | Dielectric properties (at $T_{Max}$ ) |               | Dielectric properties (at 25 °C) |               | Diffusivity ( $\gamma$ ) (at 1 kHz) |
|---------------|------------|---------------------------------------|---------------|----------------------------------|---------------|-------------------------------------|
|               |            | $\epsilon_r$                          | $\tan \delta$ | $\epsilon_r$                     | $\tan \delta$ |                                     |
| PZT           | –          | >29000                                | 0.010         | 1100                             | 0.006         | –                                   |
| 0.1PMN–0.9PZT | –          | $\sim 3700$                           | 0.020         | 700                              | 0.020         | –                                   |
| 0.3PMN–0.7PZT | 160        | 3800                                  | 0.030         | 1400                             | 0.030         | 1.62                                |
| 0.5PMN–0.5PZT | 115        | 6100                                  | 0.045         | 2200                             | 0.040         | 1.83                                |
| 0.7PMN–0.3PZT | 71         | 10100                                 | 0.057         | 5600                             | 0.057         | 1.80                                |
| 0.9PMN–0.1PZT | 16         | 10700                                 | 0.077         | 10300                            | 0.001         | 1.56                                |
| PMN           | –8         | 7600                                  | 0.073         | 6000                             | 0.001         | 1.49                                |

with temperature, but are nearly independent of frequency, except in the vicinity of the phase transformation temperature. This is a typical characteristic of ferroelectric ceramics with a long-range ordered structure.<sup>1,8</sup> The Curie temperature ( $T_C$ ) for PZT ceramic is not determinable in this study as a result of limited range of the measuring set-up, though is widely known to be close to 400 °C.<sup>2,3,11,20</sup> While PZT exhibits a normal ferroelectric behavior, PMN is a well-known relaxor ferroelectric material as a result of a short-range ordered structure with a nanometer scale heterogeneity in composition.<sup>8</sup> In typical relaxor ferroelectrics, both dielectric constant ( $\epsilon_r$ ) and dielectric loss tangent ( $\tan \delta$ ) exhibit strong temperature–frequency dependence below the transition temperature, as shown in Fig. 3(d) for PMN ceramic.<sup>3,11</sup> In this case, the temperatures of maximum dielectric constant and dielectric loss tangent are shifted to higher temperature with increasing frequency. The maximum value of the dielectric constant decreases with increasing frequency, while that of the dielectric loss tangent increases. The dielectric properties then become frequency independence above the transition temperature.<sup>1,8</sup> When PMN is added to form the binary system with PZT, the dielectric behavior is shifted towards that of relaxor materials, in which the dielectric properties vary significantly with frequency below the phase transition temperature. The results shown in Fig. 3(a–d) clearly indicate such a trend. However, with relatively small amount of PMN added, such as in 0.1PMN–0.9PZT and 0.3PMN–0.7PZT ceramics, the dielectric properties exhibit a mixture of both normal and relaxor characteristics, for instance as shown in Fig. 3(b) in which the transition temperature is not shifted as much as for other relaxor-like ceramics. Similar tendency has also been observed in several prior investigations.<sup>1,4,8</sup> It should also be noted here that the dielectric properties in all ceramics increase significantly at high temperature as a result of thermally activated space charge conduction.

The degree of broadening or diffuseness in the observed dielectric variation could be estimated with the diffusivity ( $\gamma$ ) using the expression  $\ln(1/\epsilon_r - 1/\epsilon_{\max})$  versus  $(T - T_{\max})^\gamma$ . The value of  $\gamma$  can vary from 1, for normal ferroelectrics with a normal Curie–Weiss behavior, to 2, for completely disordered relaxor ferroelectrics.<sup>21–23</sup> The plots shown in Fig. 4 show that the variation is very linear. The mean value of the diffusivity ( $\gamma$ ) is extracted from these plots by fitting a linear equation. The values of  $\gamma$  listed in Table 2 vary between 1.49 and 1.83, which confirms that diffuse phase transitions occur in PMN–PZT ceramics with a high degree of disorder. However, the trend opposes the expectation. It is expected that PMN should have the highest degree of disorder, but the calculation somewhat indicates that PZT addition leads to higher degree of disorder (the value of  $\gamma$  increases from 1.49 for PMN to 1.83 for 0.5PMN–0.5PZT). Since for a perovskite ferroelectric it is established that the diffuseness could be caused by the decrease of grain size, the observed difference of the degree of the diffuseness could be a result of the grain size variation.<sup>1</sup> Therefore, this effect can partly be the cause of the increase of the diffusivity when PZT is added to

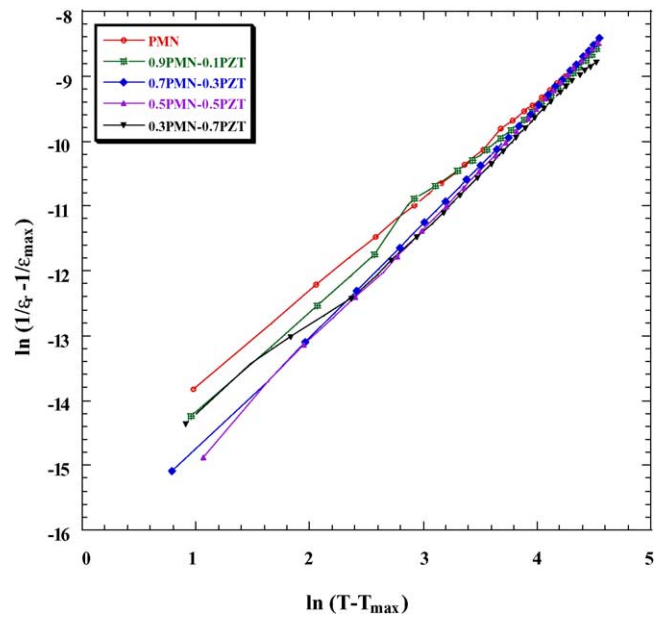


Fig. 4. Variation of  $\ln(1/\epsilon_r - 1/\epsilon_{\max})$  vs.  $\ln(T - T_{\max})$  of (x)PMN–(1 – x)PZT ceramics in the paraelectric region at 1 kHz.

PMN since the average grain size decreases from 3.25  $\mu\text{m}$  in PMN to 1.90  $\mu\text{m}$  in 0.5PMN–0.5PZT. Additionally, the reason for the observation could also be to a degree attributed to a formation of secondary pyrochlore phase in high PMN content compositions.

Furthermore, as shown in Table 2 since the transition temperature of PMN is very low ( $\sim 8$  °C at 1 kHz) and its maximum dielectric constant is very high ( $\sim 7600$  at 1 kHz), it is also expected to observe that the transition temperature decreases and the maximum dielectric constant increases with increasing amount of PMN in the system.<sup>8</sup> This is clearly evident in Fig. 5. Fig. 6 shows that the transition temperature (at

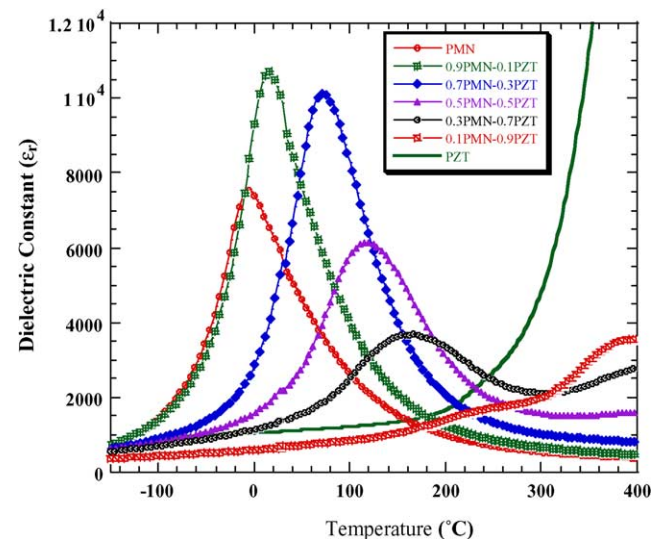


Fig. 5. Temperature dependence of dielectric constant of (x)PMN–(1 – x)PZT ceramics (measured at 1 kHz).

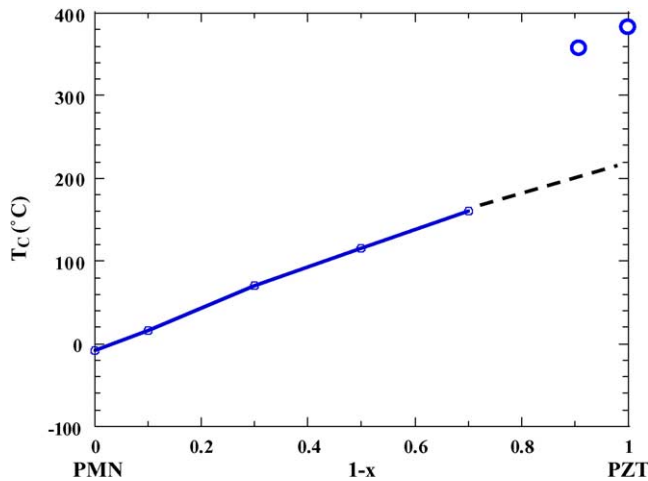


Fig. 6. Curie temperature of  $(x)$ PMN– $(1-x)$ PZT ceramics (measured at 1 kHz).

1 kHz for this case) moves towards lower temperature almost linearly with the average rate of  $\sim -2.4$  °C/mol% as the molar fraction of PMN in the composition increases. However, it is noted that this relationship does not cover the compositions 0.1PMN–0.9PZT and pure-phase PZT, which are expected to have the transition temperature near 400 °C, shown in Fig. 6 as open circles. The reason is not clearly known, but could be attributed to the pseudo-binary nature of this system, as described in the earlier publication,<sup>6</sup> in which PZT and PMN do not form a complete solid solution, but rather a composite. In this case, depending upon the composition the properties of main constituent strongly govern the properties of the system. Moreover, it could also be a discontinuity at the composition of the morphotropic phase boundary, as previously described in literatures.<sup>1,4,5</sup> It is of very interest to see that a previous investigation by Koval et al.<sup>1</sup> reported that the transition temperature of PMN–PZT system moved towards lower temperature with the rate of  $-4.1$  °C/mol% of PMN in the composition. The difference is believed to be the influence of the Zr/Ti ratio in PZT because in the work by Koval et al.<sup>1</sup> the Zr/Ti ratio is 47/53 while in our study the ratio is 52/48.

Fig. 7 illustrates a series of polarization ( $P$ – $E$ ) hysteresis loops for the  $(x)$ PMN– $(1-x)$ PZT ceramics. It is clearly evident that the shape of  $P$ – $E$  loops varies greatly with the ceramic compositions. The polarization loop of PZT is well-developed showing large remnant polarization ( $P_r$ : remaining polarization when electric field is decreased to zero). The hysteresis loop is of a typical “square” form as a result of domain switching in an applied field. This is a typical characteristic of a phase that contains long-range interaction between dipoles in the ferroelectric micro-domain state.<sup>8</sup> This confirms that PZT is of a normal ferroelectric phase. From the loop, the remnant polarization  $P_r$  and the coercive field  $E_C$  (indicating and electric field required to zero the polarization) are determined to be  $12.5$   $\mu\text{C}/\text{cm}^2$  and  $10$  kV/cm, respectively, as listed in Table 3.

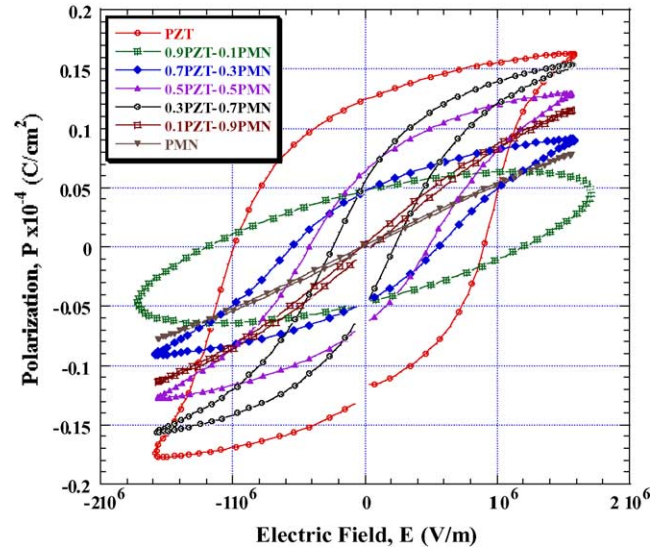


Fig. 7.  $P$ – $E$  hysteresis loops of  $(x)$ PMN– $(1-x)$ PZT ceramics.

The ferroelectric characteristic of the ceramics can be assessed with the hysteresis loop squareness ( $R_{sq}$ ) which is typically understood to be the ratio of  $P_r/P_s$  where  $P_r$  is the remnant polarization at zero electric field and  $P_s$  is the saturated polarization obtained at some finite field strength below the dielectric breakdown. Jin et al.<sup>24</sup> used the loop squareness to measure not only the deviation in the polarization axis but also that in the electric field axis with the empirical expression  $R_{sq} = (P_r/P_s) + (P_{1.1E_C}/P_r)$ , where  $P_{1.1E_C}$  is the polarization at the field equal to  $1.1E_C$ .<sup>24</sup> For the ideal square loop,  $R_{sq}$  is equal to 2.00. As listed in Table 3, the value of  $R_{sq}$  decreases from 1.16 for PZT to 0.53 for 0.7PMN–0.3PZT. This clearly quantifies that when more PMN content is added to the system, the hysteresis curves become more of “slim” hysteresis loops, a characteristic of the suppressed ferroelectric interaction.<sup>1,8</sup> This is typically found in the relaxor ferroelectrics with polar nano-regions. These results clearly indicate that an addition of PMN induces the relaxor behaviors of PMN into the PMN–PZT ceramic system. This also has resulted in decreasing of the values of both  $P_r$  and  $E_C$ , as seen in Table 3, due to an increased pseudo-cubic non-ferroelectric phase content.<sup>6,8</sup> These values agree fairly well with the values reported in previous investigations.<sup>8–10,25</sup> However, a

Table 3  
Ferroelectric properties of  $(x)$ PMN– $(1-x)$ PZT ceramics

| Ceramic       | Ferroelectric properties (at 25 °C) |                                     |               | Loop squareness ( $R_{sq}$ ) |
|---------------|-------------------------------------|-------------------------------------|---------------|------------------------------|
|               | $P_r$ ( $\mu\text{C}/\text{cm}^2$ ) | $P_s$ ( $\mu\text{C}/\text{cm}^2$ ) | $E_C$ (kV/cm) |                              |
| PZT           | 12.5                                | 16.5                                | 10            | 1.16                         |
| 0.1PMN–0.9PZT | –                                   | –                                   | –             | –                            |
| 0.3PMN–0.7PZT | 5.0                                 | 9.5                                 | 5.5           | 0.78                         |
| 0.5PMN–0.5PZT | 6.5                                 | 13.0                                | 4.5           | 0.77                         |
| 0.7PMN–0.3PZT | 5.2                                 | 15.5                                | 2.3           | 0.53                         |
| 0.9PMN–0.1PZT | –                                   | –                                   | –             | –                            |
| PMN           | –                                   | –                                   | –             | –                            |

variation in the values is probably due to different poling conditions and processing methods.<sup>26</sup> Therefore, it can be concluded that the ferroelectric properties of the ceramics in PMN–PZT system move gradually from the normal ferroelectric state in PZT to the relaxor ferroelectric state in PMN. It is also of interest to observe that the hysteresis loop of 0.1PMN–0.9PZT ceramic is not fully saturated. This is due to the limited capability of the measuring set-up used. However, it is expected that ceramics with chemical formulae in the vicinity of this composition should possess better ferroelectric properties, as reported in recent publications.<sup>1,8,12</sup> There could also be a reason of conduction lost that leads to elliptical loop in this composition.<sup>23</sup>

#### 4. Conclusion

The  $(x)\text{Pb}(\text{Mg}_{1/3}\text{Nb}_{2/3})\text{O}_3-(1-x)\text{Pb}(\text{Zr}_{0.52}\text{Ti}_{0.48})\text{O}_3$  (where  $x = 0, 0.1, 0.3, 0.5, 0.7, 0.9$ , and  $1.0$ ) ceramic composites are prepared from PZT and PMN powders by a mixed-oxide method. The dielectric properties of the ceramics are determined as functions of both temperature and frequency with an automated dielectric measurement system, while the ferroelectric properties are measured by means of a modified Sawyer-Tower circuit. The dielectric measurement takes place over the temperature range of  $-150^\circ\text{C}$  and  $400^\circ\text{C}$  with measuring frequency between 100 Hz and 1 MHz. The results indicate that the dielectric properties of the pure-phase PZT and PMN follow that of normal and relaxor ferroelectric behaviors, respectively. The dielectric behaviors of the 0.1PMN–0.9PZT and 0.3PMN–0.7PZT ceramics are more of normal ferroelectrics, while the other compositions are obviously of relaxor ferroelectrics. However, it is very of interest to see that the degree of diffuseness increases slightly when PZT is added to PMN. It is also observed that the transition temperature decreases and the maximum dielectric constant increases with increasing amount of PMN in the system. From the  $P$ – $E$  hysteresis loops, it is shown that the ferroelectric properties of the ceramics in PMN–PZT system move gradually from the normal ferroelectric state in PZT ceramic, with large  $P_r$  and  $E_C$  values, to the relaxor ferroelectric state in PMN ceramic.

#### Acknowledgment

The authors would like to express their gratitude for financial support from the Thailand Research Fund (TRF).

#### References

- Koval, V., Alemany, C., Briancin, J. and Brunckova, H., Dielectric properties and phase transition behavior of  $(x)\text{PMN}-(1-x)\text{PZT}$  ceramic systems. *J. Electroceram.*, 2003, **10**, 19–29.
- Haertling, G. H., Ferroelectric ceramics: history and technology. *J. Am. Ceram. Soc.*, 1999, **82**, 797–818.
- Cross, L. E., Review: ferroelectric materials for electromechanical transducer applications. *Mater. Chem. Phys.*, 1996, **43**, 108–115.
- Ouchi, H., Nagano, K. and Hayakawa, S., Piezoelectric properties of  $\text{Pb}(\text{Mg}_{1/3}\text{Nb}_{2/3})\text{O}_3$ – $\text{PbTiO}_3$ – $\text{PbZrO}_3$  solid solution ceramics. *J. Am. Ceram. Soc.*, 1965, **48**, 630–635.
- Ouchi, H., Piezoelectric properties and phase relations of  $\text{Pb}(\text{Mg}_{1/3}\text{Nb}_{2/3})\text{O}_3$ – $\text{PbTiO}_3$ – $\text{PbZrO}_3$  ceramics with barium or strontium substitutions. *J. Am. Ceram. Soc.*, 1968, **51**, 169–176.
- Yimnirun, R., Ananta, S., Meechoowas, E. and Wongsanmai, S., Effect of uniaxial stress on dielectric properties of lead magnesium niobate-lead zirconate titanate ceramics. *J. Phys. D: Appl. Phys.*, 2003, **36**, 1615–1619.
- He, L. X., Gao, M., Li, C. E., Zhu, W. M. and Yan, H. X., Effects of  $\text{Cr}_2\text{O}_3$  addition on the piezoelectric properties and microstructure of  $\text{PbZr}_x\text{Ti}_y(\text{Mg}_{1/3}\text{Nb}_{2/3})_{1-x-y}\text{O}_3$  ceramics. *J. Eur. Ceram. Soc.*, 2001, **21**, 703–709.
- Koval, V., Alemany, C., Briancin, J., Brunckova, H. and Saksl, K., Effect of PMN modification on structure and electrical response of  $x\text{PMN}-(1-x)\text{PZT}$  ceramic systems. *J. Eur. Ceram. Soc.*, 2003, **23**, 1157–1166.
- Shilnikov, A. V., Sopit, A. V., Burkhanov, A. I. and Luchaninov, A. G., The dielectric response of electrostrictive  $(1-x)\text{PMN}-x\text{PZT}$  ceramics. *J. Eur. Ceram. Soc.*, 1999, **19**, 1295–1297.
- Burkhanov, A. I., Shilnikov, A. V., Sopit, A. V. and Luchaninov, A. G., Dielectric and electromechanical properties of  $(1-x)\text{PMN}-x\text{PZT}$  ferroelectric ceramics. *Phys. Solid State.*, 2000, **42**, 936–943.
- Cross, L. E., Relaxor ferroelectrics. *Ferroelectrics*, 1987, **76**, 241–267.
- Shaw, J. C., Lin, K. S. and Lin, I. N., Dielectric behavior at morphotropic phase boundary for PMN–PZT ceramics. *Scripta Mater.*, 1993, **29**, 981–986.
- Abe, Y., Yanagisawa, Y., Kakagawa, K. and Sasaki, Y., Piezoelectric and dielectric properties of solid solution of  $\text{PbZrO}_3$ – $\text{PbTiO}_3$ – $\text{Pb}(\text{Mg}_{1/3}\text{Nb}_{2/3})\text{O}_3$  system prepared by wet–dry combination method. *Solid State Commun.*, 2000, **113**, 331–334.
- Stringfellow, S. B., Gupta, S., Shaw, C., Alcock, J. R. and Whatmore, R. W., Electrical conductivity control in uranium-doped  $\text{PbZrO}_3$ – $\text{PbTiO}_3$ – $\text{Pb}(\text{Mg}_{1/3}\text{Nb}_{2/3})\text{O}_3$  pyroelectric ceramics. *J. Eur. Ceram. Soc.*, 2002, **22**, 573–578.
- Whatmore, R. W., Molter, O. and Shaw, C. P., Electrical properties of Sb and Cr-doped  $\text{PbZrO}_3$ – $\text{PbTiO}_3$ – $\text{PbMg}_{1/3}\text{Nb}_{2/3}\text{O}_3$  ceramics. *J. Eur. Ceram. Soc.*, 2003, **23**, 721–728.
- Wang, C. H., The microstructure and characteristics of 0.875PZT–0.125PMN ceramics with addition of Pb-based flux. *J. Eur. Ceram. Soc.*, 2002, **22**, 2033–2038.
- Jiang, Q., *Electrically Induced Fatigue Effects and Reliability in Piezoelectric and Electrostrictive Ceramics*. Ph.D. Thesis, The Pennsylvania State University, 1992.
- Park, S. E. and Shrout, T. R., Ultrahigh strain and piezoelectric behavior in relaxor based ferroelectric single crystals. *J. Appl. Phys.*, 1997, **82**, 1804.
- Park, J. H., Yoon, K. H. and Kang, D. H., Dielectric and electrical properties of preferentially (111) oriented Zr-rich  $0.1\text{Pb}(\text{Mg}_{1/3}\text{Nb}_{2/3})\text{O}_3$ – $0.9\text{Pb}(\text{Zr}_x\text{Ti}_{1-x})\text{O}_3$  thin films by chemical solution deposition. *Thin Solid Films*, 2001, **396**, 84–89.
- Las, W. C., Spagnol, P. D., Zaghete, M. A. and Cilense, M., Electrical characterization of lead zirconate titanate prepared by organic solution route. *Ceram. Int.*, 2001, **27**, 367.
- Shannigrahi, S. R., Tay, F. E. H., Yao, K. and Choudhary, R. N. P., Effect of rare earth (La, Nd, Sm, Eu, Gd, Dy, Er and Yb) ion substitutions on the microstructural and electrical properties of sol–gel grown PZT ceramics. *J. Eur. Ceram. Soc.*, 2004, **24**, 163–170.
- Rai, R. and Sharma, S., Structural and dielectric properties of (La Bi) modified PZT ceramics. *Solid State Commun.*, 2004, **129**, 305–309.
- Alberta, E. F. and Bhalla, A. S., Low-temperature property investigation of the lead indium-niobate-lead nickel-niobate solid solution. *J. Phys. Chem. Solids*, 2002, **63**, 1759–1769.

24. Jin, B. M., Kim, J. and Kim, S. C., Effects of grain size on the electrical properties of  $\text{PbZr}_{0.52}\text{Ti}_{0.48}\text{O}_3$  ceramics. *Appl. Phys.*, 1997, **A 65**, 53–56.
25. Murty, K. V. R., Murty, S. N., Mouli, K. C. and Bhanumathi, A., Domain orientation and piezoelectric properties of Ag-doped PMN–PZT ceramics. *Proc. IEEE Intl. Symp. Appl. Ferroelectr.*, 1992, **1**, 144–147.
26. Qui, W. and Hng, H. H., Effects of dopants on the microstructure and properties of PZT ceramics. *Mater. Chem. Phys.*, 2002, **75**, 151–156.